

Identification of FUSE-binding proteins as interacting partners of TIA proteins

Françoise Rothé^a, Cyril Gueydan^a, Eric Bellefroid^b, Georges Huez^a, Véronique Kruys^{a,*}

^a Laboratoire de Chimie Biologique, Institut de Biologie et de Médecine Moléculaires, Université Libre de Bruxelles, 6041 Gosselies, Belgium

^b Laboratoire d'Embryologie Moléculaire, Institut de Biologie et de Médecine Moléculaires, Université Libre de Bruxelles, 6041 Gosselies, Belgium

Received 7 February 2006

Available online 28 February 2006

Abstract

TIA-1 and TIAR are closely related RNA-binding proteins involved in several mechanisms of RNA metabolism, including alternative hnRNA splicing and mRNA translation regulation. In particular, TIA-1 represses tumor necrosis factor (TNF) mRNA translation by binding to the AU-rich element (ARE) present in the mRNA 3' untranslated region. Here, we demonstrate that TIA proteins interact with FUSE-binding proteins (FBPs) and that *fbp* genes are co-expressed with *tia* genes during *Xenopus* embryogenesis. FBPs participate in various steps of RNA processing and degradation. In Cos cells, FBPs co-localize with TIA proteins in the nucleus and migrate into TIA-enriched cytoplasmic granules upon oxidative stress. Overexpression of FBP2-KH3 RNA-binding domain fused to EGFP induces the specific sequestration of TIA proteins in cytoplasmic foci, thereby precluding their nuclear accumulation. In cytosolic RAW 264.7 macrophage extracts, FBPs are found associated in EMSA to the TIA-1/TNF-ARE complex. Together, our results indicate that TIA and FBP proteins may thus be relevant biological involved in common events of RNA metabolism occurring both in the nucleus and the cytoplasm.

© 2006 Elsevier Inc. All rights reserved.

Keywords: RNA binding proteins; Stress granules

TIA-1 and TIAR are related proteins belonging to the large family of RNA-binding proteins (RB-Ps) containing RNA recognition motifs (RRMs). RRM domains correspond to ~100 amino acid domains that have conserved hexamer and octamer peptide sequence motifs (RNP2 and RNP1) which mediate the physical contact with RNA. TIA-1 and TIAR contain three N-terminal RRM domains and a C-terminal auxiliary domain. The highest degree of identity between these related proteins is observed at the level of the RRM domains (more than 90% identity) whereas the C-terminal regions diverge more significantly (51% identity). Both TIA-1 and TIAR are expressed as two isoforms, resulting from the alternative splicing of a common precursor transcript, leading to the inclusion or exclusion of 11 or

17 amino acid peptides in RRM2 or RRM1 of TIA-1 and TIAR, respectively [1].

TIA-1 and TIAR are nucleo-cytoplasmic shuttling proteins, which mostly accumulate in the nucleus in somatic cells. While their nuclear accumulation was shown to be mediated by the second RRM and the first half of the auxiliary domain, their export from the nucleus is depending on the RNA-binding capacity of the third RRM [46]. In the nucleus, these proteins act as RNA-splicing regulators of a series of alternatively spliced pre-mRNAs (Fas, msl-2, FGFR-2, and calcitonin/CGRP) [2–4]. Indeed, TIA-1 was shown to promote the recruitment of U1 small nuclear ribonucleoprotein to a class of weak 5' splice sites by binding to uridine-rich sequences immediately downstream from the 5' splice site [5].

In the cytoplasm, TIA-1 and TIAR have been shown to regulate the translation of various mRNAs by binding to AU-rich elements (AREs) located in these mRNA 3'

* Corresponding author. Fax: +322 6509800.

E-mail address: vkruys@ulb.ac.be (V. Kruys).

untranslated regions (3'UTRs). This is the case of mRNAs encoding TNF- α , cyclooxygenase-2 (Cox-2), human matrix metalloproteinase-13 (HMMP-13), and β 2-adrenergic receptor [6–9]. In addition to the translational silencing of selected cytoplasmic transcripts, both TIA-1 and TIAR participate in the cellular response to environmental stress as they migrate in cytoplasmic foci called stress granules (SGs) [10,11]. Originally found in plant cells [12,13], these structures are also formed in mammalian cells upon exposure to different stresses. These foci constitute reservoirs of sequestered mRNAs maintained in an untranslated status. Indeed, mRNAs located in SGs are associated with a non-canonical 48S pre-initiation complex that lacks the translation initiation factor eIF-2 as well as the 60S large ribosomal subunit. In fact, the formation of SGs can be induced by the phosphorylation of the α subunit of eIF-2 which blocks translation initiation by reducing the availability of the eIF-2-GTP-tRNAi-Met ternary complex that loads initiator methionine onto the small ribosomal subunit [10,14]. Very recently, TIAR was shown to bind single-stranded thymidine-rich sequences and this with a 6-fold higher affinity than to RNA. Interestingly, TIAR can be displaced from single-stranded DNA by active transcription through the binding site, thereby suggesting that TIAR can shuttle between DNA and RNA ligands [15].

In this report, we demonstrated the interaction of TIA-1 and TIAR with FUSE-binding proteins (FBPs) and show that *tia* and *fbp* genes are co-expressed during *Xenopus* early development. Our results suggest that TIA and FBPs proteins participate in common events of RNA metabolism occurring both in the nucleus and the cytoplasm.

Materials and methods

Materials. Enzymes were purchased from Invitrogen and Roche. Oligonucleotides were purchased from Sigma or Genset. The anti-Flag M2 monoclonal antibody was purchased from Sigma-Aldrich. The anti-TIA-1, anti-TIAR, and anti-FBP polyclonal antibodies were purchased from Santa Cruz Biotechnology. The biotin-labeled Sm antibody was a product of Neomarkers. The Alexa 594-coupled donkey anti-mouse IgG and donkey anti-goat IgG secondary antibodies were products of Molecular Probes. The Texas red-coupled donkey anti-goat secondary antibody and streptavidin-Cy5 were kindly provided by F. Bex. The donkey anti-Smad2 antibody was kindly provided by C. Van Lint.

DNA constructs. The yeast two-hybrid vectors pPC97 and pPC86, respectively, carrying *LEU2* and *TRP1* selection markers [16] and the pPC97-NTPIE8 construct, used as positive control for reporter gene activation, were kindly given by Dr. D. Perez-Morga and have previously been described [17]. The entire coding region of *Xenopus laevis* TIA-1 was amplified by PCR and inserted into the *SmaI/SpeI* sites of the pPC97 vector. Partial xTIA-1 coding sequences containing nucleotides (1–890 for TIA-1 Δ CT; 277–1167 for TIA-1 Δ RRM1; 1–277 and 584–1167 for TIA-1 Δ RRM2; 1–584 and 891–1167 for TIA-1 Δ RRM3) were amplified by PCR and then subcloned into the *SmaI/SpeI* sites of the pPC97 vector. The pGEX4T2-TIA-1 construct was obtained by inserting the entire TIA-1 coding region into the *BamHI* and *EcoRI* sites of the pGEX4T2 vector (Amersham Biosciences). The pCMVSPORT6-flagTIA-1 construct was generated by inserting the entire TIA-1 coding region in-frame with the flag tag into the *XbaI* and *HindIII* sites of the pCMVSPORT6 vector. The pCMVSPORT6-FBP1 and FBP2 constructs were obtained by inserting FBP1 and FBP2 ORFs into the *XbaI* and *HindIII* sites of the pCMV-

SPORT6 vector. The pCS2-flagBoip construct is a gift of Van Wayenberg and has previously been described [18]. DNA constructs used to express EGFP hybrid proteins were generated by introducing PCR-amplified fragments corresponding to TIA-1, FBP1, and FBP2 coding sequences between *XhoI* and *HindIII* sites of the pECFP and pEYFP vectors. The pEGFP-C2-TIA-1 construct was previously described [46]. The pEGFP-KH3 plasmid was obtained by introducing a PCR fragment corresponding to the third KH domain (aa 322–386) of FBP2 into *EcoRI* and *BamHI* sites of the pEGFP-C2 plasmid (Clontech).

The yeast two-hybrid screening. All experiments were performed in the yeast strain AH109 harboring the reporter genes *HIS3*, *ADE2*, and *LacZ* [19]. This strain has been transformed with pPC97-TIA-1 construct according to the lithium acetate method. The AH109 strain expressing the Gal4 DBD-TIA-1 fusion protein was then transformed with a *Xenopus* neurula stage cDNA library [18]. Positive clones were selected for their ability to grow on medium lacking leucine, tryptophan, histidine, and adenine and assayed for β -galactosidase activity using the method described below. Plasmids were isolated from positive yeast cells and the cDNAs were sequenced.

Quantification of β -galactosidase activity. Yeast cultures were grown overnight in synthetic dropout medium lacking leucine and tryptophan, and were diluted fivefold in YEPD medium, and incubated until the optical density at 600 nm (OD_{600}) reached 0.5–0.8. After one wash in buffer 1, pH 7.3 (100 mM Hepes, 150 mM NaCl, 5 mM aspartate, 1% BSA, and 0.05% Tween 20) and resuspension in 100 μ l buffer 1, the yeast cells were lysed by two freeze-thaw cycles using liquid nitrogen. Cell lysates were then resuspended in 0.7 ml of buffer 1 containing 2.23 mM chlorophenol red- β -D-galactopyranoside (CPRG), a substrate of β -galactosidase. Upon apparition of the yellow/red colour, the reaction was stopped by the addition of 500 μ l of 3 M ZnCl₂ and the OD_{578} was determined. A β -Gal unit is defined as $OD_{578} \times 1000 / (t \times 9 \times OD_{600})$ where t is the reaction time (min).

GST pull-down assay. The prokaryotic expression plasmids pGex4T-1, pGex4T-2-TIA-1, and pGEX2T-TIAR were transformed into the DH10B *Escherichia coli* strain. Overnight cultures were diluted sixfold in LB medium containing ampicillin (100 μ g/ml) and further incubated until the OD_{600} reached 0.7. Expression of the GST fusion protein was induced with 1 mM isopropyl-1-thio- β -D-galactopyranoside for 3 h 30 min. The cells were then harvested, washed with phosphate-buffered saline, and lysed by sonication. The GST and the GST fusion protein were purified by incubation with glutathione-Sepharose 4B beads (Amersham Biosciences) for 2 h at 4 °C. The beads were washed three times with PBS. The amount of GST and GST-TIA-1 bound to the beads was quantified by SDS-PAGE and Coomassie blue staining. Equal amounts of fusion proteins were incubated with in vitro transcribed and translated [³⁵S]-methionine labeled FBP1 and FBP2 (in vitro transcription-translation; Promega). After gentle overnight shaking at 4 °C in NETN binding buffer (50 mM NaCl, 20 mM Tris-HCl, pH 8, 1 mM EDTA, 0.5% Nonidet P-40, and protease inhibitors (Roche)) in the absence or presence of RNase A (1 μ g/ml), the beads were washed three times in PBS. Finally, bound proteins were analyzed by SDS-PAGE and autoradiography. To verify the RNase treatment, total RNA present in the supernatant of the beads was recovered by phenol/chloroform extractions and precipitation to be analyzed by agarose gel electrophoresis and ethidium bromide staining.

Embryos and in situ hybridization. *Xenopus* embryos were obtained from adult frogs by hormone-induced egg-laying and in vivo fertilization using standard methods and staged according to Nieuwkoop and Faber [20]. Whole-mount in situ hybridization was performed as described using digoxigenin-labeled antisense RNA probes [21]. To produce the TIA-1 probe, the cDNA cloned into pCS107 (EST 3199481) was linearized by *Sall* and transcribed with T7. To produce the TIAR probe, the cDNA cloned into pBSK (EST 3380028) was linearized with *EcoRI* and transcribed with T3. To produce the FBP1 and FBP2 probes, the cDNAs identified in the yeast two-hybrid screen cloned into pSK+ vectors were linearized with *Sall* and transcribed with T3. For sections, embryos after the completion of the whole-mount procedure were gelatin-embedded and vibratome-sectioned at 30 μ m thickness.

RT-PCR. Total RNA from the different embryonic stages studied was extracted using NETS buffer method (300 mM NaCl, 50 mM Tris, pH 7.5,

1 mM EDTA, and 1% SDS), reverse-transcribed using ThermoScript RT-PCR System (Life Technologies) according to the manufacturer's instructions, and analyzed by PCR.

Cell culture and transient transfection. Cos-7 cells were grown in Dulbecco's modified Eagle's medium (Gibco-BRL) containing 10% fetal bovine serum (Gibco-BRL), penicillin (50 U/ml), streptomycin (50 mg/ml), and L-glutamine (2 mM). For fluorescence microscopy, Cos-7 cells were grown overnight on coverslips and transfected using FUGENE-6 reagent (Roche) according to the manufacturer's instructions. Two micrograms of DNA was transfected in 2×10^5 cells with 6 μ l FUGENE-6. Cells were fixed for 24 or 48 h after transfection. Where indicated, the cells were treated with 500 μ M sodium arsenite (Sigma) for 30 min.

Co-immunoprecipitation. Cos-7 cells were transiently transfected using FUGENE-6 reagent (Roche) according to the manufacturer's instructions. pCS2-flag-BOIP [18] and pCMVSPORT6-Flag-TIA-1 plasmids were transfected either with pCMVSPORT6-FBP1 or pCMVSPORT6-FBP2 in 7.5×10^5 cells. Twenty-four hours after transfection, cells were washed twice in ice-cold PBS and lysed in IP buffer (50 mM Tris-HCl, pH 7.8, 100 mM NaCl, 0.05% NP40, and protease inhibitors (Roche)) for 30 min at 4 °C. Flagged-proteins were immunoprecipitated by incubating protein extract (2 mg) with Anti-Flag M2 (15 μ l) affinity gel (Sigma) for 2 h at 4 °C in the absence or presence of RNase A. The beads were then washed twice in IP buffer. Bound proteins were eluted in Laemmli gel sample buffer, separated by electrophoresis on a 12.5% SDS-polyacrylamide gel, and transferred to nitrocellulose for Western blot analysis. Western blot analysis of FBPs and Flagged proteins was performed with anti-FBP antibody (0.4 μ g/ml) and M2 monoclonal anti-Flag antibody (2.3 μ g/ml), respectively.

Fluorescence microscopy. The subcellular distribution of EGFP hybrid proteins was analyzed 24 h after transfection. Cells grown on coverslips were washed three times with PBS, fixed in 3.7% paraformaldehyde in PBS for 10 min at room temperature (RT), incubated in 125 mM glycine for 10 min, washed three times with PBS and mounted. For epifluorescence analysis, DAPI (100 pg/ml) was added to the mounting medium. The cells were then analyzed by epifluorescence (Leica DM 4000B) or confocal fluorescence microscopy (Zeiss LSM510). For immunofluorescence experiments, the subcellular distribution of TIA-1, FBPs, Sm, and FLAG-tagged proteins was analyzed according to the same procedure, except that after fixation in 3.7% paraformaldehyde and incubation in 125 mM glycine, cells were permeabilized in PBS, Triton X-100 0.5% for 5 min at 4 °C, were washed twice in PBS and were incubated in PBS, 0.5% gelatin and 0.25% bovine serum albumin for 30 min at RT. The coverslips were incubated with the primary antibody diluted in the former solution for 1 h at RT (anti-TIA-1, dilution 1:50; anti-FBPs, dilution 1:50; anti-FLAG, dilution 1:2000; and anti-Sm, dilution 1:100). The samples were then washed three times with PBS, 0.2% gelatin and incubated for 1 h with the secondary antibody (Alexa 594- or Texas Red-coupled donkey anti-goat to detect TIA-1 and FBPs diluted 10,000 \times and 200 \times , respectively) and Alexa 594-coupled donkey anti-mouse to detect FLAG-tagged proteins (dilution 1:25,000), and Cy5-coupled streptavidin to detect Sm antibody (dilution 1:1000). The samples were then washed three times in PBS, 0.2% gelatin and mounted before fluorescence analysis.

Electrophoretic mobility shift assay and supershift. Cytosolic S100 extracts from RAW264.7 mouse macrophages were incubated with a 3' TNF probe containing or not the ARE as described previously [22]. Supershifts with anti-TIA-1, anti-FBP or control (anti-MAD2) antibodies were performed by incubating 20 μ g of S100 extract with 0.2 μ g antibody for 25 min on ice in a total volume of 15 μ l before the electrophoretic mobility shift assay (EMSA). The EMSAs were electrophoresed on non-denaturing 3.5% polyacrylamide gels.

Results

TIA-1 and TIAR interact with FUSE-BP1 and 2

To characterize the role of TIA-1 protein in particular during embryogenesis, we have isolated by mining the

Xenopus EST database *Xenopus* TIA-1 and TIAR cDNA clones (Accession Nos.: AJ416632 and AJ416631). Sequence alignments show that *Xenopus* TIA-1 and TIAR have 84% and 88% identity with the mouse homolog (data not shown). To search for TIA-1 interacting partners, the sequence encoding *Xenopus* TIA-1 was cloned by PCR downstream from the Gal4 DNA-binding domain (DBD) in the yeast two-hybrid vector pPC97 and was used to screen a *Xenopus* neurula egg cDNA library cloned downstream from the Gal4 activation domain (AD) in the yeast two-hybrid vector pPC86 [18]. 10^5 transformants growing on α LeuTrp medium were screened with the bait. Ninety positive clones were isolated after plating on α LeuTrpHis selective medium and 40 of them were further isolated after plating on α LeuTrpHisAde medium. Out of these 40 candidates, six remained positive for β -galactosidase expression. The cDNAs of the six positive clones were purified and re-introduced in yeast cells in combination with empty or TIA-1 encoding pPC97 plasmids to verify the necessity of Gal4 DBD-TIA-1 expression for their growth on α LeuTrpHisAde selective medium. Four candidates came out positive from this screening. Sequence analysis of the four cDNAs revealed that three of them encoded the *Xenopus* homolog of human FUSE-BP2 (FBP2, also named KSRP) (75% identity) and the fourth one encoded the homolog of human FUSE-BP1 (FBP1) (78% identity). Fig. 1 shows that β -galactosidase activity is significantly increased only upon co-expression of Gal4 DBD-TIA-1 with Gal4 AD-FBP1 or AD-FBP2, thereby confirming the necessity of the two proteins to activate the *LacZ* reporter gene.

As TIAR is structurally and functionally highly related to TIA-1, we determined its capacity to interact with FBP1 and 2 by the same procedure. We observed that likewise to TIA-1, TIAR interacted with FBP1 and FBP2 (Fig. 1).

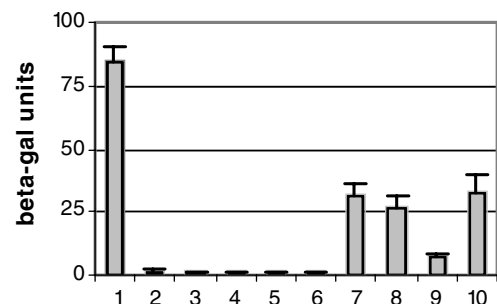


Fig. 1. Identification of FBP1 and FBP2 as partners of TIA-1 and TIAR proteins in a yeast two-hybrid assay. pPC97, pPC97-TIA-1 or pPC97-TIAR constructs were introduced in AH109 yeast strain by transformation together with pPC86, pPC86-FBP1 or pPC86-FBP2. Transformants were grown in Dropout medium lacking leucine and tryptophan. *LacZ* reporter gene expression was measured by β -galactosidase assay. The data are representative of two independent experiments. Transformed DNAs: (1) pPC97-NT-PIE8 used as a positive control of reporter gene activation. (2) pPC97 + pPC86, (3) pPC97 + pPC86-FBP1, (4) pPC97 + pPC86-FBP2, (5) pPC97-TIA-1 + pPC86, (6) pPC97-TIAR + pPC86, (7) pPC97-TIA-1 + pPC86-FBP1, (8) pPC97-TIA-1 + pPC86-FBP2, (9) pPC97-TIAR + pPC86-FBP1, (10) pPC97-TIAR + pPC86-FBP2.

To further confirm the specificity of the interaction between TIA-1 and FBP1 and FBP2, GST pull-down assays were performed. FBP1 and 2 were synthesized by *in vitro* translation in rabbit reticulocyte lysate in the presence of [35 S]-methionine and were incubated in the presence of equal amounts of GST or GST-TIA-1 proteins immobilized on glutathione–Sepharose beads (Fig. 2A). As shown in Fig. 2B (top panel), FBP1 and 2 were pulled down by GST-TIA-1 but not by GST alone. As TIA-1 and FBPs are all RNA-binding proteins, we performed the same assay in the presence of RNase to exclude the role of RNA intermediates in the interactions (Fig. 2B, bottom panel). The RNase activity was verified by analyzing the degradation of the reticulocyte lysate RNA present in the binding assay (Fig. 2C).

Similar results were obtained from co-immunoprecipitation assays using lysates from Cos cells transfected with Flag-tagged TIA-1 and FBP1 or 2 expression vectors (Fig. 2D). In this assay, the specificity of the interactions was monitored by evaluating the capacity of an unrelated protein, Boip [18], to pull down FBP1 and 2 proteins. Of note, both exogenous and endogenous FBP1 and 2 were co-immunoprecipitated by Flag-TIA-1 protein in the presence (Fig. 2D) or the absence of RNase (data not shown).

Finally, the interaction of TIAR with FBPs was also confirmed by GST pull-down assays performed in the same conditions as with GST-TIA-1 (Fig. 2E).

Altogether, these results confirmed the capacity of TIA proteins to interact with FBPs.

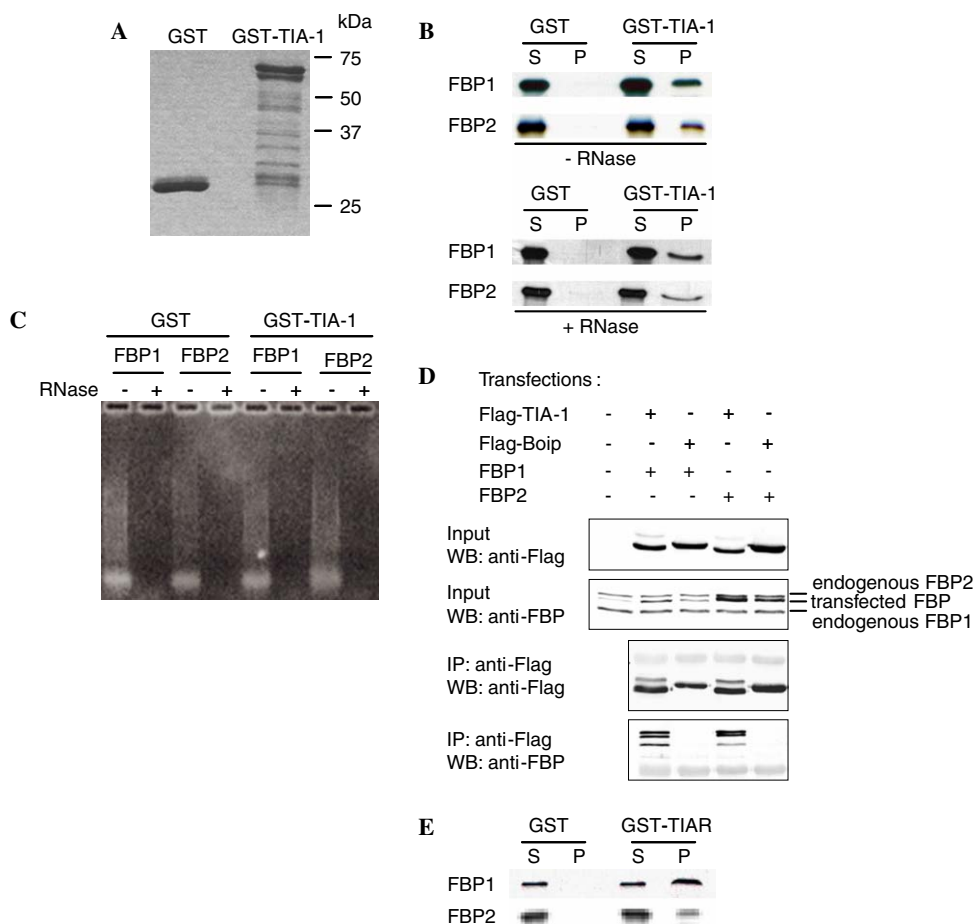


Fig. 2. Interaction of xFBP1 and xFBP2 with xTIA-1 in an *in vitro* GST pull-down assay and by co-immunoprecipitation. (A) Quantitation of GST and GST-TIA-1 proteins immobilized on the glutathione–Sepharose beads by SDS–PAGE and Coomassie blue staining. (B) Equivalent amounts of GST and GST-TIA-1 bound on the glutathione–Sepharose beads were incubated with *in vitro* translated 35 S-labeled FBP1 and FBP2. Pelleted proteins (P) and 1% of the pull-down supernatants (S) were analyzed by SDS–PAGE and autoradiography. Experiments were performed in the absence or presence of RNase A. (C) Verification of the RNase treatment by agarose gel electrophoresis and ethidium bromide staining of the RNA present in the binding reaction (see Materials and methods). (D) Co-immunoprecipitation of FBP1 and FBP2 with flag-TIA-1. Cos-7 cells were transiently transfected with DNA constructs expressing flag-TIA-1 or flag-Boip (control) in combination with FBP1- or FBP2-expressing constructs. Cells were lysed and flag-tagged proteins were immunoprecipitated with Sepharose beads coupled with M2 anti-flag antibody. Input (Input) and immunoprecipitates (IP) were analyzed by SDS–PAGE and Western blotting (WB) with anti-flag or anti-FBP antibodies. Transfected DNAs are indicated. The experiments were performed in the absence or presence (data not shown) of RNase A in the cell lysate. (E) GST pull-down assay performed with GST-TIAR. The experiment was performed as described in (B).

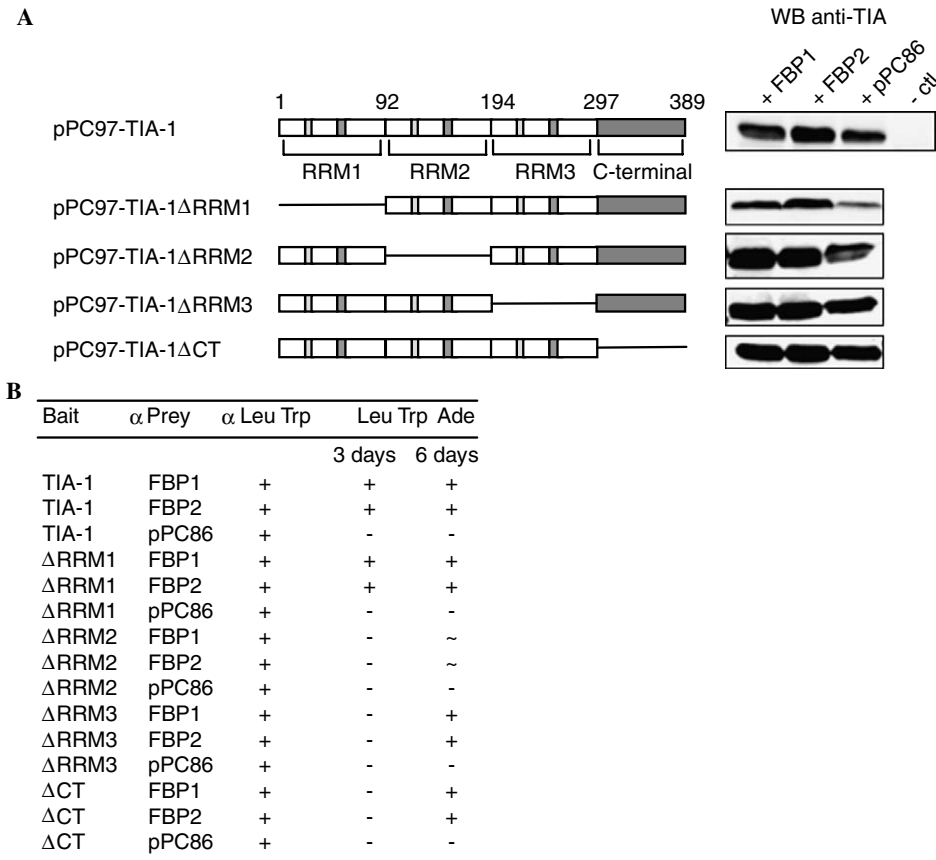


Fig. 3. Identification of TIA-1 domains involved in the interactions with FBP1 and FBP2 using the yeast two-hybrid system. (A) Schematic representation of TIA-1 and various deletion mutants in fusion with the Gal4 DBD. The AH109 yeast strain was transformed with pPC97 TIA-1 or mutant constructs (prey) together with pPC86 vector, pPC86-FBP1 or pPC86-FBP2 (bait). The expression of TIA-1 and the deletion mutants was verified by Western blot analysis using the anti-TIA-1 (C-20) except for the C-terminal-deleted mutant which was detected by the cross-reacting anti-TIAR (N-19) antibody. (B) Protein interactions were measured by evaluating yeast growth after 3 and 6 days on α LeuTrpAde selective medium.

Identification of interacting domains within TIA-1

We then attempted to identify the domains within TIA-1 that are involved in the interaction with FBP1 and 2. Therefore, we generated several deletion mutants of TIA-1 in the two-hybrid vector pPC97 (Fig. 3A) and tested their ability to interact with FBP1 and 2 in the yeast two hybrid system. This analysis was performed by evaluating the growth capacity of the yeast transformants on α LeuTrpAde medium after 3 and 6 days at 30 °C. In parallel, the expression of the different mutants was verified by Western blot (Fig. 3A). As shown in Fig. 3B, RRM1 of TIA-1 can be dispensed without affecting the interactions. In contrast, the removal of any of the other RRMs or of the auxiliary domain led to a major growth arrest after 3 days as no colonies appeared for these mutants. After 6 days however, some growth differences appeared between them as colonies appeared with the mutants lacking RRM3 or the auxiliary domain while very tiny colonies only appeared for the mutant lacking RRM2. These results indicate that both RRM2 and 3 as well as the auxiliary domain are involved in the interaction with FBP1 and 2, RRM2 playing a major role in the interaction.

TIA-1, TIAR, FBP1, and FBP2 are co-expressed during *Xenopus* embryogenesis

To determine whether TIA-1, TIAR, FBP1, and FBP2 are co-expressed in the embryo, we first determined their temporal expression patterns by reverse transcriptase polymerase chain reaction (RT-PCR). We found that all four genes are expressed both maternally and zygotically in the developing embryo. As determined by comparison to histone H4 that is uniformly expressed throughout *Xenopus* development, their expression appeared stronger from neurula stage (stage 14) (Fig. 4A). Western blot analysis of TIA-1, TIAR, FBP1, and FBP2 protein accumulation revealed that the four proteins are also produced at all stages analyzed, a higher amount of protein being detected from neurula stage (data not shown). To elucidate their spatial expression, we performed whole-mount in situ hybridizations (Fig. 4B). Consistent with the RT-PCR and Western blot analysis, we detected expression of all four genes at all stages examined. At blastula/gastrula stages (stages 9–10.5), TIA-1, TIAR, FBP1, and FBP2 are expressed throughout the animal pole (ap). At neurula stage (stages 14–16), their transcripts were predominantly

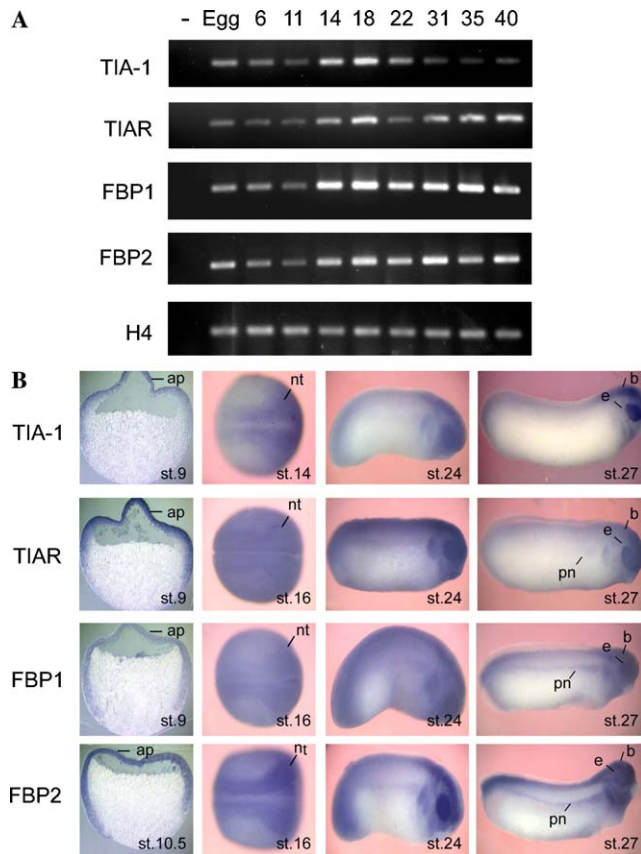


Fig. 4. TIA-1, TIAR, FBP1, and FBP2 are co-expressed during *Xenopus* embryogenesis. (A) TIA-1, TIAR, FBP1, and FBP2 temporal expression patterns were analyzed by RT-PCR. The embryogenesis stages studied are indicated above each lane. The negative control corresponds to PCR which has been made without template. Histone H4 was used as internal control. (B) TIA-1, TIAR, FBP1, and FBP2 spatial expressions were performed by whole-mount in situ hybridizations.

detected throughout the developing neural tube (nt). At tailbud and tadpole stages (stages 24–27), their expression was detected in the brain (b), eyes (e), cranial neural crest cells, and the pronephros (pn). FBP1 and FBP2 show highly similar expression patterns to those of TIA-1 and TIAR, suggesting that they may be relevant partners during embryogenesis.

Co-localization of TIA-1, FBP1, and FBP2 in the nucleus of somatic cells

TIA-1 and FBP1 and 2 mostly accumulate in the nuclear compartment, TIA-1 being more abundant in the cytoplasmic fraction than FBPs [23,24]. To further characterize TIA-1/FBPs interaction, we compared their subcellular localization by fluorescence microscopy. For this purpose, we generated DNA constructs to express TIA-1 and FBP1 or 2 in fusion with the EGFP variants, ECFP and EYFP, respectively. These constructs were transfected into Cos-7 cells and the subcellular distribution of the fusion proteins was analyzed by fluorescence confocal microscopy. As previously described, EGFP-

tagged TIA-1 and FBPs mostly accumulated in the nucleus of the cells. However, while some TIA-1 is observed in the cytoplasm, the presence of FBPs in this compartment is undetectable (Fig. 5A). Of note, TIA-1 and FBP1 and 2 are concentrated in hundreds of dots throughout the nucleus and are also present in a diffuse pattern in the surrounding nucleoplasm. Moreover, these proteins appear to be excluded from nucleoli. We then performed co-localization studies by co-expressing ECFP-TIA-1 with EYFP-FBP1 or EYFP-FBP2. ECFP-TIA-1 co-localized perfectly with both EYFP-FBP1 (Fig. 5B) and EYFP-FBP2 (Fig. 5C) in the nucleus. To verify the physiological significance of the co-localization experiments using EGFP-tagged proteins, we transfected either ECFP-TIA-1 or EYFP-FBP1 and 2 alone in Cos-7 cells and compared their nuclear distribution to endogenous FBP1 and 2 or TIA-1, respectively. Same results as in earlier experiments were obtained, thereby confirming the perfect co-localization of TIA-1 and FBPs in the nucleus (Fig. 6).

The nuclear distribution of TIA and FBPs proteins was further characterized by comparing the localization of ECFP-TIA-1 and EYFP-FBP1 to that of snRNP using anti-Sm antibodies [25]. As reported in previous studies [26], the snRNP antigens are concentrated in discrete regions within the nucleus and are also present in a diffuse pattern in the nucleoplasm. The superposition of the fluorescent signals revealed that both ECFP-TIA-1 and EYFP-FBP1 co-localized with Sm antigens except in the Sm-rich speckles (Fig. 7). Altogether, these results indicate that TIA and FBP proteins share an identical nuclear distribution which is only partially overlapping with Sm antigens.

Co-localization of TIA-1 and FBPs in cytoplasmic stress granules

Although immunofluorescence experiments suggested an exclusive FBPs staining in the nucleus, biochemical studies demonstrated the presence of these proteins in the cytoplasm (Fig. 4) [27,28]. Besides, TIA-1 is known to migrate in cytoplasmic granules upon cellular stress [10]. We therefore investigated whether FBPs also migrated in such foci in response to oxidative stress induced by arsenite. As earlier described, TIA-1 is concentrated in stress granules (SGs) in response to arsenite. Interestingly, similar foci were observed upon oxidative stress after staining of the cells with anti-FBP (Fig. 8A). To confirm that FBP-containing foci corresponded to SGs, Cos-7 cells were transfected with the EGFP-TIA-1 construct and were subsequently treated with arsenite. Cells were then stained with anti-FBP antibody and analyzed by fluorescence microscopy to observe EGFP-TIA-1 (green) and FBPs (red) subcellular distribution. As shown in Fig. 8B, FBPs co-localized in EGFP-TIA-1 cytoplasmic foci, thereby confirming the migration of FBPs into SGs upon oxidative stress.

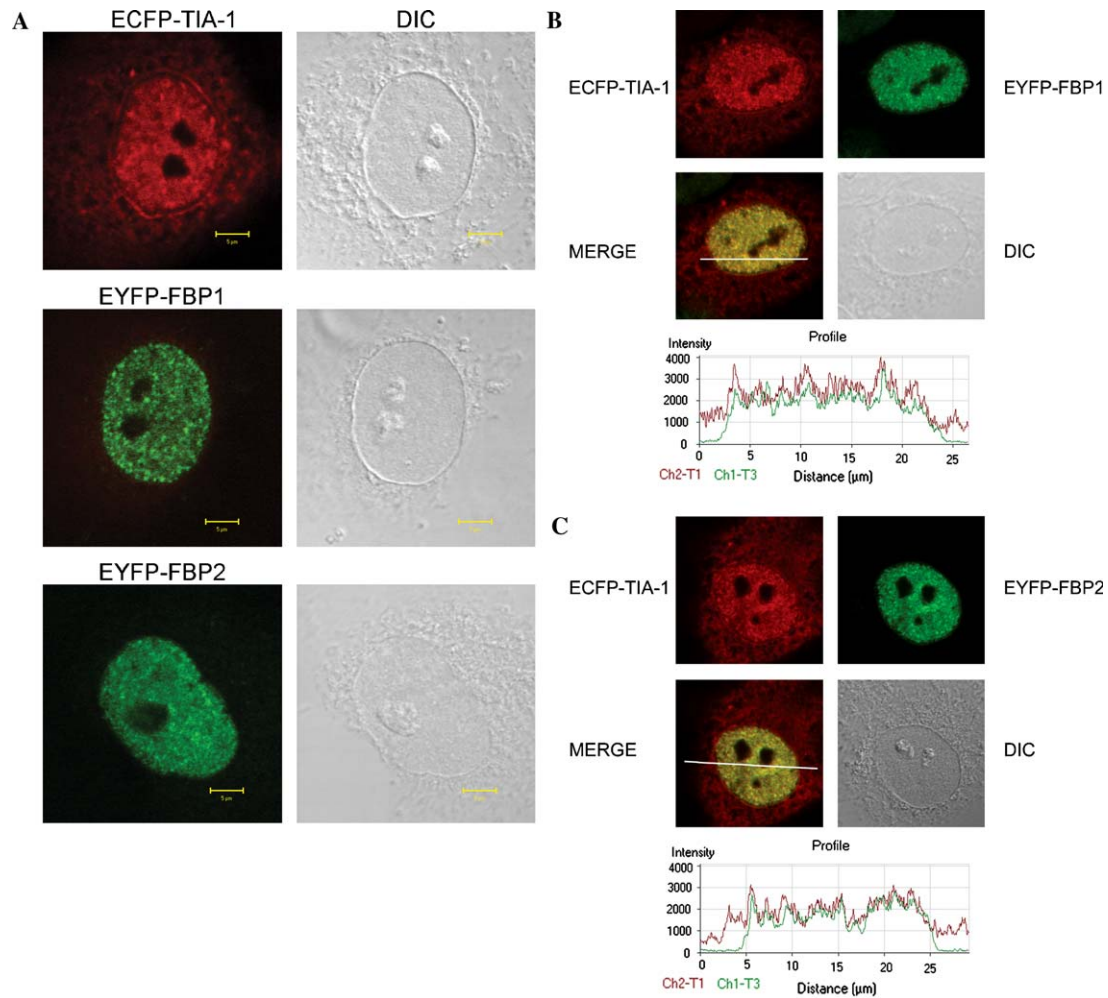


Fig. 5. (A) Subcellular localization of ECFP-TIA-1, EYFP-FBP1, and EYFP-FBP2 in somatic cells. Cos-7 cells were transiently transfected with pECFP-TIA-1 (red), pEYFP-FBP1, and pEYFP-FBP2 (green) constructs, respectively. Twenty-four hours post-transfection, the cells were fixed and the protein distribution was analyzed by confocal fluorescence microscopy (left panels). The right panels (DIC) show the differential interference contrast images of the cells. (B,C) ECFP-TIA-1 co-localizes with EYFP-FBP1 (B) and EYFP-FBP2 (C) in the nucleus of somatic cells. Cos-7 cells were transiently transfected with pECFP-TIA-1 and pEYFP-FBP1 constructs (B) or with pECFP-TIA-1 and pEYFP-FBP2 constructs (C). Twenty-four hours post-transfection, the cells were fixed and the protein distribution was analyzed by confocal fluorescence microscopy. The merged images show the perfect co-localization of ECFP-TIA-1 and EYFP-FBP1 (or EYFP-FBP2) in the nucleus (yellow staining). The profiles reveal the red and green fluorescence intensities along a line crossing the cell. The bottom right panels (DIC) show the differential interference contrast image of the cells. (For interpretation of the references to colour in this figure legend, the reader is referred to the web version of this paper.)

The expression of a FBP2 mutant specifically mislocalizes TIA-1 and TIAR in cytoplasmic foci

As TIA-1 and FBPs perfectly co-localized in the nucleus and shared the ability to migrate into SGs, we investigated whether the expression of truncated forms of KSRP/FBP2 modified the subcellular distribution of TIA-1. In particular, we tested the ability of a fusion protein made of the EGFP and the third KH RNA-binding motif (KH3) to mislocalize TIA-1. Indeed, the functional analysis of KSRP/FBP2 different domains revealed the ability of KH3 domain to recruit the RNA degradative activities without being able to bind to RNA [29]. DNA constructs encoding EGFP alone or in fusion with KH3 were transfected into Cos cells. After transfection, cells were stained with anti-TIA-1 antibody and analyzed by fluorescence micros-

copy to observe EGFP (green) and TIA-1 (red) subcellular distribution. We observed that the EGFP-KH3 protein distributed both in the nucleus and the cytoplasm. In the latter compartment, however, EGFP-KH3 was both diffusely distributed and concentrated in small cytoplasmic foci. Interestingly, the expression of EGFP-KH3 led to the sequestration of endogenous TIA-1 in these cytoplasmic foci, thereby precluding its nuclear accumulation (Fig. 9A). TIA-1 mislocalization was clearly dependent on the expression of KH3 domain as EGFP alone did not disturb its distribution (Fig. 9B). Moreover, while EGFP-KH3 similarly mislocalized TIAR (Fig. 9A), for which we showed the ability to interact with FBPs, no such effect was observed for Boip, whose cytoplasmic distribution remained diffuse (Fig. 9C) [18]. Altogether, these results indicated that the expression of FBP2 KH3 domain

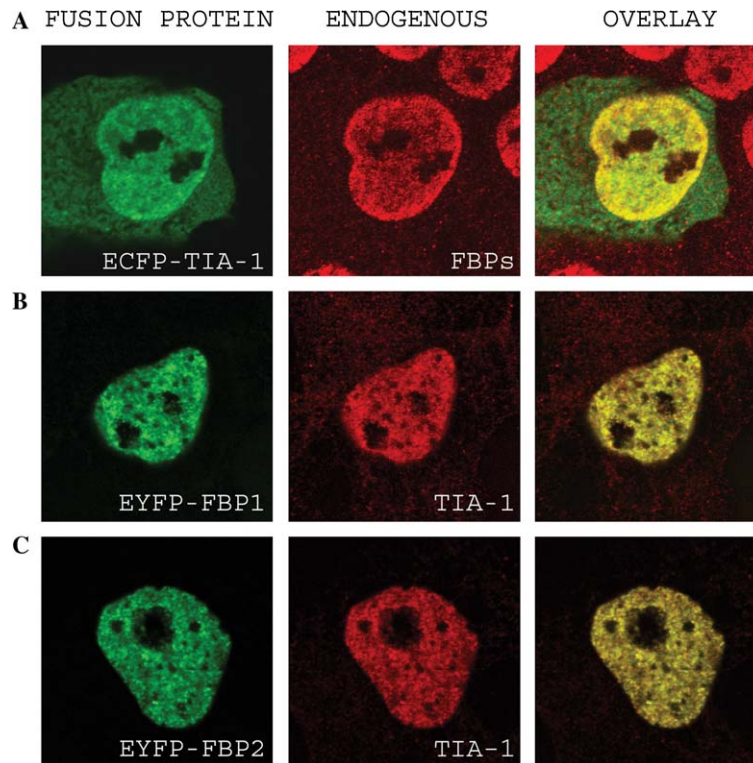


Fig. 6. ECFP-TIA-1 and EYFP-FBP fusion proteins co-localize in the nucleus with endogenous FBPs and TIA-1, respectively. Cos-7 cells were transiently transfected with pECFP-TIA-1 (A), pEYFP-FBP1 (B), and pEYFP-FBP2 (C) constructs. Twenty-four hours after transfection, the cells were fixed, immunostained with anti-FBP (A) or anti-TIA-1 (B,C) antibodies, and analyzed by confocal microscopy. The EGFP-fusion proteins appear in green and endogenous proteins in red. The overlay images show the co-localization of the proteins appearing in yellow. (For interpretation of the references to colour in this figure legend, the reader is referred to the web version of this paper.)

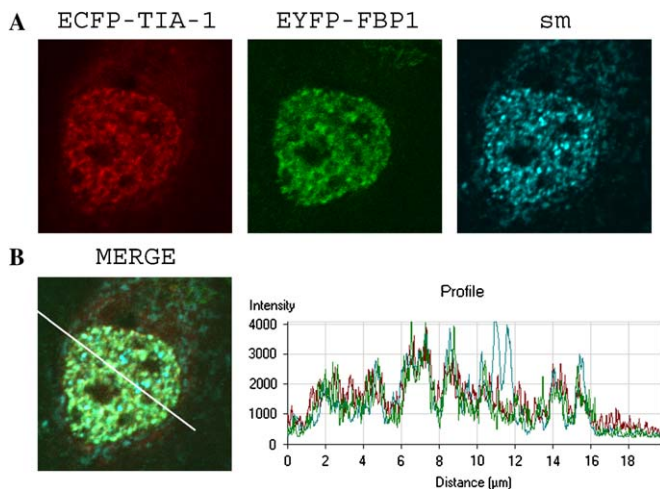


Fig. 7. TIA-1 and FBP1 partially co-localize with Sm antigens present on snRNP. Cos-7 cells were transiently transfected with pECFP-TIA-1 (red) and pEYFP-FBP1 (green) constructs. Twenty-four hours post-transfection, the cells were fixed, stained with anti-Sm antibody (blue) and the protein distribution was analyzed by confocal fluorescence microscopy (A). The merged images show the partial co-localization of the proteins. The profile reveals the red, green, and blue fluorescence intensities along a line crossing the cell (B). (For interpretation of the references to colour in this figure legend, the reader is referred to the web version of this paper.)

Presence of FBPs in TNF ARE/TIA-1 RNA-protein complex

In addition to its role in the general translational arrest induced by environmental stresses, TIA-1 participates in specific mRNA translational silencing via its ARE-binding capacity [6]. Several studies also revealed the capacity of KSRP/FBP2 to promote the ARE-dependent mRNA degradation by recruiting the exosome and the poly(A) ribonuclease (PARN) [27,29]. In particular, Linker et al. [28] demonstrated the functional importance of KSRP in the ARE-dependent degradation of inducible nitric oxide synthase (iNOS) mRNA in epithelial cells. To assess the relevance of FBP/TIA-1 interactions in TNF ARE-dependent post-transcriptional regulation, we first investigated the presence of FBPs in previously described TNF ARE/TIA-1 complexes [6]. For this purpose, cytosolic extracts of RAW264.7 macrophage cells were prepared and were immunoblotted with anti-TIA-1 and anti-FBP antibodies to verify their content in TIA-1 and FBPs (Fig. 10A). These extracts were subsequently used in gel shift assays with riboprobes corresponding to TNF mRNA 3' UTR with or without ARE (Fig. 10B). As previously observed, the incubation of TNF 3'UTR riboprobe with RAW 264.7 extract led to the formation of a low mobility complex which is supershifted by anti-TIA-1 antibody. This complex required the ARE as it was almost undetectable with the riboprobe lacking

in fusion with EGFP specifically sequestered TIA-1 and TIAR in cytoplasmic granules, thereby inhibiting their nuclear accumulation.

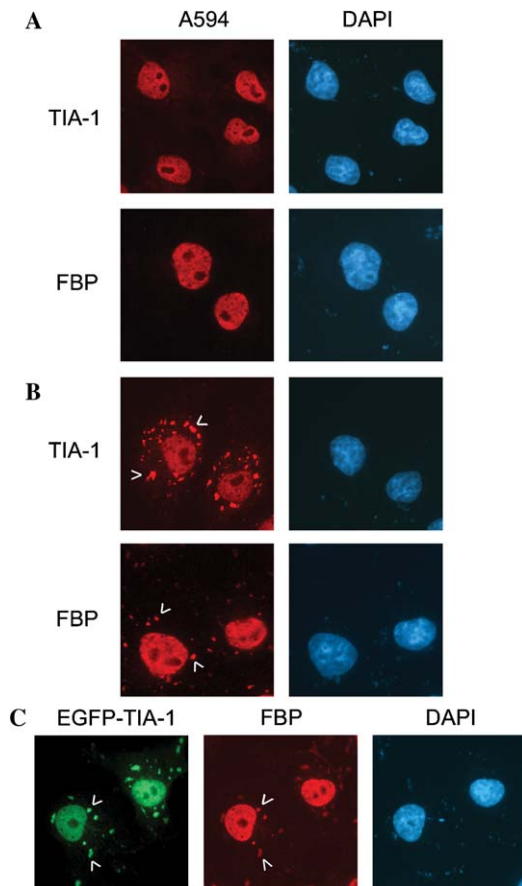


Fig. 8. FBPs accumulate in stress granules after arsenite treatment. Cos-7 cells were cultured in the absence (A) or presence (B) of arsenite (0.5 mM, 30 min) before immunostaining with anti-TIA-1 or anti-FBP antibodies. (C) Cos-7 cells were transiently transfected with pEGFP-TIA-1 construct. Twenty-four hours after transfection, cells were cultured in the presence of arsenite (0.5 mM, 30 min) before immunostaining with anti-FBP antibody. EGFP-TIA-1 (green) and FBPs (red) were analyzed by fluorescence microscopy. Nuclei were detected by DAPI staining. Stress granules are indicated by arrows. (For interpretation of the references to colour in this figure legend, the reader is referred to the web version of this paper.)

the ARE (Fig. 10C). The addition of anti-FBP antibody to the extract before incubation with TNF probe led also to the supershift of the TNF ARE/TIA-1 complex, thereby demonstrating the presence of FBPs in this complex. The ability of TIA-1 and at least one of the FBPs to concomitantly associate with TNF ARE suggests a potential role of TIA-1/FBPs interaction in the ARE-dependent post-transcriptional regulation of TNF mRNA.

Discussion

In this study, we demonstrated that TIA-1 and TIAR interact with both FBP1 and 2. FBP1 was identified initially as a nuclear single-stranded DNA-binding protein that regulated the expression of *c-myc* via binding to the far upstream sequence element (FUSE) of the *c-myc* locus [30]. Later on, members of the FBP family have been implicated in various aspects of mRNA metabolism. As such,

FBP2/KSRP mediates the neuron-specific N1 exon inclusion in *c-src* transcript [31] and interacts with sequences involved in the cytoplasmic localization of microtubule-associated protein 2 and β actin mRNAs [23,32]. FBP1 and 2 also bind to AU-rich elements (ARE) present in several transient mRNAs and the capacity of FBP2/KSRP to induce iNOS mRNA destabilization was clearly demonstrated [28]. Functional analyses revealed that the degradative activity of FBP2/KSRP relies on its capacity to recruit the poly(A) ribonuclease and the exosome, a multiprotein complex mediating mRNA 3' to 5' degradation [27,29].

We also show that *Xenopus* homologs of *tia* and *fbp* genes are expressed throughout embryogenesis and that they are predominantly transcribed in the developing nervous system (Fig. 4). The expression profile we observed supports the idea that post-transcriptional control of gene expression plays an important role during early neural development.

TIA-1 and FBPs perfectly co-localize in the nuclear compartment of somatic cells. Indeed, TIA-1 and FBP1/2 appear concentrated in hundreds of dots throughout the nucleoplasm above a homogenous but less abundant nuclear distribution (Figs. 5 and 6). Additional co-localization experiments with Sm antigens (snRNPs) revealed that TIA and FBPs proteins co-localize with Sm antigens except in Sm-enriched nuclear speckles (Fig. 7). These speckles also enriched in the non-snRNP SC-35 antigen (data not shown) are mostly considered as storage sites for splicing components [33]. TIA and FBPs proteins do not co-localize with C-terminal phosphorylated polymerase II, a marker for active transcription sites (data not shown) [34]. These observations suggest that TIA and FBPs proteins most probably interact during splicing events rather than in transcriptional processes. In this regard, it is worth noting that the KSRP-containing complex, which mediates *c-src* neuron-specific N1 exon inclusion, includes an unidentified protein of 43 kDa, a molecular weight compatible with those of TIA proteins [35]. During embryogenesis, the expression of N1 exon-containing *c-src* transcript begins early in neural development and is restricted to the neural plate in *Xenopus* embryos [36]. This expression profile coincides with those of TIA and FBPs proteins (Fig. 4). It is thus possible that the N1 exon inclusion into *c-src* transcripts in neural tissues relies on a combined action of FBPs and TIA proteins.

We showed that FBPs migrated into TIA-1-containing SGs upon oxidative stress (Fig. 8). SGs have been recently described as storage and triage cytoplasmic reservoirs from which untranslated mRNAs are either routed back to polysomes or are transferred to processing bodies in which they are degraded [37]. TIA-1 was reported to be a major mediator of SG formation. Indeed, a TIA-1 truncation mutant lacking its RNA-binding domains prevents the arsenite-induced assembly of SGs [11]. ARE-binding proteins other than TIA-1 and TIAR are found in SGs. This is the case of tristetraprolin (TTP) [38] and the cold-induced RNA-binding protein (CIRP) (unpublished data), which

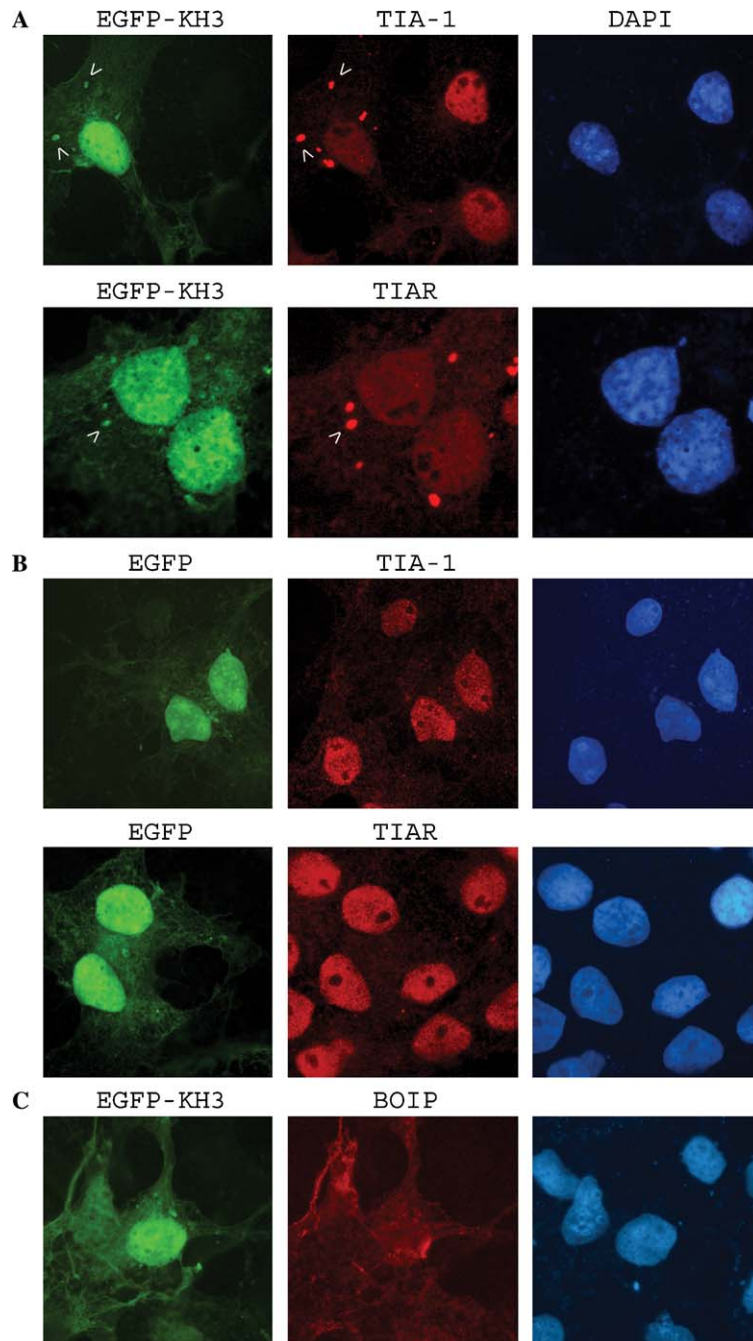


Fig. 9. The expression of a FBP2 mutant specifically mislocalizes TIA-1 and TIAR in cytoplasmic foci. (A,B) Localization of TIA-1 and TIAR in Cos cells transfected with EGFP-FBP2-KH3 and EGFP, respectively. Left panels: localization of EGFP-FBP2-KH3 (A) and EGFP (B); middle panels: endogenous TIA-1 and TIAR; right panels: DAPI staining. (C) Localization of Boip in Cos cells transfected with pEGFP-C2-FBP2-KH3. Left panel, EGFP; middle panel, Boip; and right panel, DAPI staining.

interact with TIA-1 and TIAR (unpublished data). So far, it has been hypothesized that these proteins condition the routing of ARE-containing mRNAs within these stress-induced cytoplasmic structures [37]. The presence of FBPs in TIA-1-containing SGs (Fig. 8) suggests that FBPs contribute to these complex routing mechanisms of ARE-containing mRNAs within these sub-cytoplasmic structures.

The existence of an interacting event between TIA and FBPs proteins is further documented by the capacity of

FBP2 KH3 RNA-binding domain fused with EGFP to sequester TIA-1 and TIAR in cytoplasmic foci and to impair their nuclear import (Fig. 9A). Although the mechanism underlying this phenomenon remains to be investigated, TIA-1 and TIAR sequestration is specific as FBP2 KH3 does not modify the localization of other proteins (Fig. 9C).

So far, TIA proteins were shown to regulate ARE-containing genes at the level of mRNA translation, and

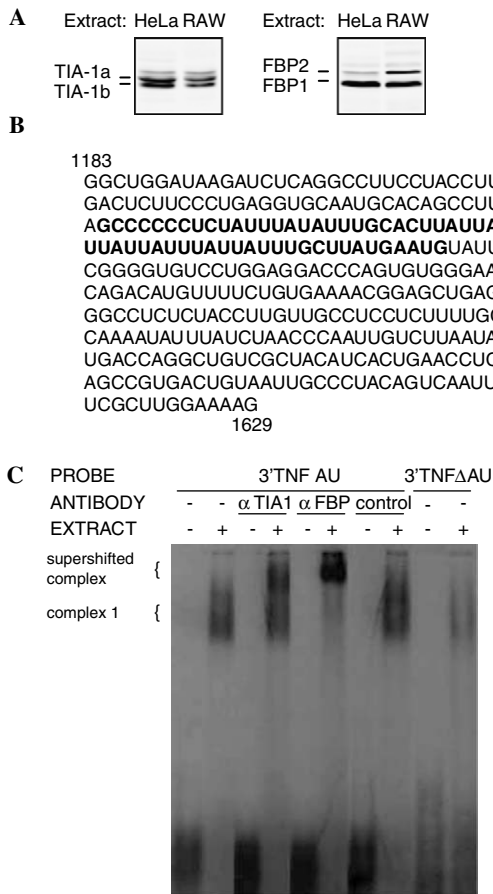


Fig. 10. (A) Western blot analysis of TIA-1 and FBPs in HeLa and RAW264.7 macrophage cytosolic extracts. (B) Sequence of TNF AU riboprobe used in EMSA. The ARE is written in bold and corresponds to the sequence deleted in TNF ΔAU probe. (C) EMSA with RAW264.7 cytosolic extract (see Materials and methods). The relative migration of complex 1 and supershifted complex 1 is indicated on the left.

KSRP at the level of mRNA stability. Our data indicate that these ARE-BPs get associated to their target RNA sequence as heterogeneous multimeric complexes. This holds true for TNF (Fig. 10) [6,39], cyclooxygenase-2 (cox-2) [40,41], and inducible NO synthase (iNOS) [28,42] AREs. Interestingly, TNF and cox-2 AREs regulate both mRNA translation and stability [43,44]. The interaction between TIA proteins and FBP2/KSRP might thus constitute a molecular link between these two regulatory mechanisms.

In addition to TIA and FBPs proteins, the TNF, cox-2, and iNOS ARE-binding complexes also contain TTP. However, while TTP promotes the degradation of TNF mRNA [45], it contributes to cytokine-induced iNOS mRNA stabilization [42]. Altogether, these observations unravel the complex RNA-protein assemblies which regulate different ARE-containing mRNAs. The complete characterization of ARE-containing mRNPs and of their dynamics will therefore provide a major breakthrough to the understanding of ARE-mediated post-transcriptional processes.

Acknowledgments

We thank Dr. Françoise Bex and Hicham Baydoun for valuable help with confocal microscopy, and Corinne Wauquier and Patrick Defrance for valuable technical assistance. This work was funded by the EC contract (QLK3-2000-00721), the Fund for Medical Scientific Research (Belgium, Grant 3.4618.01), and the “Actions de Recherches Concertées” (Grant 00-05/250). F. Rothé was supported by a ‘Fonds pour la Recherche dans l’Industrie et l’Agriculture’ grant (FRIA).

References

- [1] A.R. Beck, Q.G. Medley, S. O'Brien, P. Anderson, M. Streuli, Structure, tissue distribution and genomic organization of the murine RRM-type RNA binding proteins TIA-1 and TIAR, *Nucleic Acids Res.* 24 (1996) 3829–3835.
- [2] P. Forch, O. Puig, N. Kedersha, C. Martinez, S. Granneman, B. Seraphin, P. Anderson, J. Valcarcel, The apoptosis-promoting factor TIA-1 is a regulator of alternative pre-mRNA splicing, *Mol. Cell* 6 (2000) 1089–1098.
- [3] F. Gatto-Konczak, C.F. Bourgeois, C. Le Guiner, L. Kister, M.C. Gesnel, J. Stevenin, R. Breathnach, The RNA-binding protein TIA-1 is a novel mammalian splicing regulator acting through intron sequences adjacent to a 5' splice site, *Mol. Cell. Biol.* 20 (2000) 6287–6299.
- [4] H. Zhu, R.A. Hasman, K.M. Young, N.L. Kedersha, H. Lou, U1 snRNP-dependent function of TIAR in the regulation of alternative RNA processing of the human calcitonin/CGRP pre-mRNA, *Mol. Cell. Biol.* 23 (2003) 5959–5971.
- [5] P. Forch, O. Puig, C. Martinez, B. Seraphin, J. Valcarcel, The splicing regulator TIA-1 interacts with U1-C to promote U1 snRNP recruitment to 5' splice sites, *EMBO J.* 21 (2002) 6882–6892.
- [6] M. Piecyk, S. Wax, A.R. Beck, N. Kedersha, M. Gupta, B. Maritim, S. Chen, C. Gueydan, V. Kruys, M. Streuli, P. Anderson, TIA-1 is a translational silencer that selectively regulates the expression of TNF-α, *EMBO J.* 19 (2000) 4154–4163.
- [7] D.A. Dixon, G.C. Balch, N. Kedersha, P. Anderson, G.A. Zimmerman, R.D. Beauchamp, S.M. Prescott, Regulation of cyclooxygenase-2 expression by the translational silencer TIA-1, *J. Exp. Med.* 198 (2003) 475–481.
- [8] Q. Yu, S.J. Cok, C. Zeng, A.R. Morrison, Translational repression of human matrix metalloproteinases-13 by an alternatively spliced form of T-cell-restricted intracellular antigen-related protein (TIAR), *J. Biol. Chem.* 278 (2003) 1579–1584.
- [9] K. Kandasamy, K. Joseph, K. Subramaniam, J.R. Raymond, B.G. Tholanikunnel, Translational control of beta2-adrenergic receptor mRNA by T-cell-restricted intracellular antigen-related protein, *J. Biol. Chem.* 280 (2005) 1931–1943.
- [10] N.L. Kedersha, M. Gupta, W. Li, I. Miller, P. Anderson, RNA-binding proteins TIA-1 and TIAR link the phosphorylation of eIF-2α to the assembly of mammalian stress granules, *J. Cell Biol.* 147 (1999) 1431–1442.
- [11] N. Kedersha, M.R. Cho, W. Li, P.W. Yacono, S. Chen, N. Gilks, D.E. Golan, P. Anderson, Dynamic shuttling of TIA-1 accompanies the recruitment of mRNA to mammalian stress granules, *J. Cell Biol.* 151 (2000) 1257–1268.
- [12] L. Nover, K.D. Scharf, D. Neumann, Formation of cytoplasmic heat shock granules in tomato cell cultures and leaves, *Mol. Cell. Biol.* 3 (1983) 1648–1655.
- [13] L. Nover, K.D. Scharf, D. Neumann, Cytoplasmic heat shock granules are formed from precursor particles and are associated with a specific set of mRNAs, *Mol. Cell. Biol.* 9 (1989) 1298–1308.

- [14] N. Kedersha, S. Chen, N. Gilks, W. Li, I.J. Miller, J. Stahl, P. Anderson, Evidence that ternary complex (eIF2-GTP-tRNA(i)-Met)-deficient preinitiation complexes are core constituents of mammalian stress granules, *Mol. Biol. Cell* 13 (2002) 195–210.
- [15] E.A. Suswam, Y.Y. Li, H. Mahtani, P.H. King, Novel DNA-binding properties of the RNA-binding protein TIAR, *Nucleic Acids Res.* 33 (2005) 4507–4518.
- [16] P.M. Chevray, D. Nathans, Protein interaction cloning in yeast: identification of mammalian proteins that react with the leucine zipper of Jun, *Proc. Natl. Acad. Sci. USA* 89 (1992) 5789–5793.
- [17] D. Perez-Morga, E. Pays, A protein linked to mitochondrion development in *Trypanosoma brucei*, *Mol. Biochem. Parasitol.* 101 (1999) 161–172.
- [18] R. Van Wayenbergh, V. Taelman, B. Pichon, A. Fischer, S. Kricha, M. Gessler, D. Christophe, E.J. Bellefroid, Identification of BOIP, a novel cDNA highly expressed during spermatogenesis that encodes a protein interacting with the orange domain of the hairy-related transcription factor HRT1/Hey1 in *Xenopus* and mouse, *Dev. Dyn.* 228 (2003) 716–725.
- [19] P. James, J. Halladay, E.A. Craig, Genomic libraries and a host strain designed for highly efficient two-hybrid selection in yeast, *Genetics* 144 (1996) 1425–1436.
- [20] P.D. Nieuwkoop, J. Faber, Normal table of *Xenopus laevis* (Daudin), North Holland, Amsterdam, 1967.
- [21] H.L. Sive, R.M. Grainger, R.M. Harland, Early Development of *Xenopus laevis*. A Laboratory Manual, Cold Spring Harbor Laboratory Press, Cold Spring Harbor, NY, 2000.
- [22] C. Gueydan, L. Houzet, A. Marchant, A. Sels, G. Huez, V. Kruys, Engagement of tumor necrosis factor mRNA by an endotoxin-inducible cytoplasmic protein, *Mol. Med.* 2 (1996) 479–488.
- [23] W. Gu, F. Pan, H. Zhang, G.J. Bassell, R.H. Singer, A predominantly nuclear protein affecting cytoplasmic localization of beta-actin mRNA in fibroblasts and neurons, *J. Cell Biol.* 156 (2002) 41–51.
- [24] L. He, A. Weber, D. Levens, Nuclear targeting determinants of the far upstream element binding protein, a c-myc transcription factor, *Nucleic Acids Res.* 28 (2000) 4558–4565.
- [25] E.A. Lerner, M.R. Lerner, C.A. Janeway Jr., J.A. Steitz, Monoclonal antibodies to nucleic acid-containing cellular constituents: probes for molecular biology and autoimmune disease, *Proc. Natl. Acad. Sci. USA* 78 (1981) 2737–2741.
- [26] U. Nyman, H. Hallman, G. Hadlaczky, I. Pettersson, G. Sharp, N.R. Ringertz, Intracellular localization of snRNP antigens, *J. Cell Biol.* 102 (1986) 137–144.
- [27] C.Y. Chen, R. Gherzi, S.E. Ong, E.L. Chan, R. Raijmakers, G.J. Pruijn, G. Stoecklin, C. Moroni, M. Mann, M. Karin, AU binding proteins recruit the exosome to degrade ARE-containing mRNAs, *Cell* 107 (2001) 451–464.
- [28] K. Linker, A. Pautz, M. Fechir, T. Hubrich, J. Greeve, H. Kleinert, Involvement of KSRP in the post-transcriptional regulation of human iNOS expression-complex interplay of KSRP with TTP and HuR, *Nucleic Acids Res.* 33 (2005) 4813–4827.
- [29] R. Gherzi, K.Y. Lee, P. Briata, D. Wegmuller, C. Moroni, M. Karin, C.Y. Chen, A KH domain RNA binding protein, KSRP, promotes ARE-directed mRNA turnover by recruiting the degradation machinery, *Mol. Cell* 14 (2004) 571–583.
- [30] R. Duncan, L. Bazar, G. Michelotti, T. Tomonaga, H. Krutzsch, M. Avigan, D. Levens, A sequence-specific, single-strand binding protein activates the far upstream element of c-myc and defines a new DNA-binding motif, *Genes Dev.* 8 (1994) 465–480.
- [31] H. Min, C.W. Turck, J.M. Nikolic, D.L. Black, A new regulatory protein, KSRP, mediates exon inclusion through an intronic splicing enhancer, *Genes Dev.* 11 (1997) 1023–1036.
- [32] M. Rehbein, K. Wege, F. Buck, M. Schweizer, D. Richter, S. Kindler, Molecular characterization of MARTA1, a protein interacting with the dendritic targeting element of MAP2 mRNAs, *J. Neurochem.* 82 (2002) 1039–1046.
- [33] R.H. Singer, M.R. Green, Compartmentalization of eukaryotic gene expression: causes and effects, *Cell* 91 (1997) 291–294.
- [34] B. Chabot, S. Bisotto, M. Vincent, The nuclear matrix phosphoprotein p255 associates with splicing complexes as part of the [U4/U6.U5] tri-snRNP particle, *Nucleic Acids Res.* 23 (1995) 3206–3213.
- [35] H. Min, R.C. Chan, D.L. Black, The generally expressed hnRNP F is involved in a neural-specific pre-mRNA splicing event, *Genes Dev.* 9 (1995) 2659–2671.
- [36] J.W. Collett, R.E. Steele, Identification and developmental expression of Src+ mRNAs in *Xenopus laevis*, *Dev. Biol.* 152 (1992) 194–198.
- [37] N. Kedersha, G. Stoecklin, M. Ayodele, P. Yacono, J. Lykke-Andersen, M.J. Fitzler, D. Scheuner, R.J. Kaufman, D.E. Golan, P. Anderson, Stress granules and processing bodies are dynamically linked sites of mRNP remodeling, *J. Cell Biol.* 169 (2005) 871–884.
- [38] G. Stoecklin, T. Stubbs, N. Kedersha, S. Wax, W.F. Rigby, T.K. Blackwell, P. Anderson, MK2-induced tristetraprolin:14-3-3 complexes prevent stress granule association and ARE-mRNA decay, *EMBO J.* 23 (2004) 1313–1324.
- [39] C. Gueydan, L. Droogmans, P. Chalon, G. Huez, D. Caput, V. Kruys, Identification of TIAR as a protein binding to the translational regulatory AU-rich element of tumor necrosis factor alpha mRNA, *J. Biol. Chem.* 274 (1999) 2322–2326.
- [40] S.J. Cok, S.J. Acton, A.R. Morrison, The proximal region of the 3'-untranslated region of cyclooxygenase-2 is recognized by a multimeric protein complex containing HuR, TIA-1, TIAR, and the heterogeneous nuclear ribonucleoprotein U, *J. Biol. Chem.* 278 (2003) 36157–36162.
- [41] G. Sully, J.L. Dean, R. Wait, L. Rawlinson, T. Santalucia, J. Saklatvala, A.R. Clark, Structural and functional dissection of a conserved destabilizing element of cyclo-oxygenase-2 mRNA: evidence against the involvement of AUF-1 [AU-rich element/poly(U)-binding/degradation factor-1], AUF-2, tristetraprolin, HuR (Hu antigen R) or FBP1 (far-upstream-sequence-element-binding protein 1), *Biochem. J.* 377 (2004) 629–639.
- [42] M. Fechir, K. Linker, A. Pautz, T. Hubrich, U. Forstermann, F. Rodriguez-Pascual, H. Kleinert, Tristetraprolin regulates the expression of the human inducible nitric-oxide synthase gene, *Mol. Pharmacol.* 67 (2005) 2148–2161.
- [43] D. Kontoyiannis, M. Pasparakis, T.T. Pizarro, F. Cominelli, G. Kollias, Impaired on/off regulation of TNF biosynthesis in mice lacking TNF AU-rich elements: implications for joint and gut-associated immunopathologies, *Immunity* 10 (1999) 387–398.
- [44] D.A. Dixon, C.D. Kaplan, T.M. McIntyre, G.A. Zimmerman, S.M. Prescott, Post-transcriptional control of cyclooxygenase-2 gene expression. The role of the 3'-untranslated region, *J. Biol. Chem.* 275 (2000) 11750–11757.
- [45] E. Carballo, W.S. Lai, P.J. Blakeshear, Feedback inhibition of macrophage tumor necrosis factor-alpha production by tristetraprolin, *Science* 281 (1998) 1001–1005.
- [46] T. Zhang et al. *Journal of Cell Science*, 118 (2005) 5453–5463.